34th Annual International Conference of the IEEE EMBS
San Diego, California USA, 28 August - 1 September, 2012

Reorganization of Functional Brain Networks during the Recovery of Stroke: A Functional MRI Study*

Lin Cheng, Zhiyuan Wu, Yi Fu, Fei Miao, Junfeng Sun, *Member, IEEE*, and Shanbao Tong, Senior *Member, IEEE*

***Abstract*—Studies have demonstrated that reorganization of the cortex after stroke contributed to the recovery of motor function. However, these studies paid much more attention to the reorganization of motor-related brain regions and motor executive network which only contained tens of brain regions, ignoring the change in brain-wide network during the restoration of motor function. Based on this consideration, this paper investigated the functional reorganization of brain-wide network during the recovery after stroke from the perspective of graph theory. At four time points (less than 10 days, around 2 weeks, 1 month and 3 months) after stroke onset, we obtained the functional MRI (fMRI) data of stroke patients when they were doing finger tapping task. Based on the fMRI data, we constructed the brain-wide functional network which consisted of 264 putative functional areas for each subject at each time point. Then the topological parameters (e.g., characteristic path length and cluster coefficient) of these brain networks were examined. Results showed that the brain networks shifted towards a non-optimal topological configuration with low small-worldness during the process of recovery. And this finding may broaden our knowledge about the reorganization of brain function during recovery after stroke.**

I. INTRODUCTION

The recovery of the motor deficit due to stroke usually starts from the first several weeks post onset up to years [1]. The underlying mechanisms of this recovery have been investigated extensively, and results shows that the recovery involves the cortical reorganization in different scales [2-5]. According to functional neuroimaging studies, the cortical reorganization commonly manifests increased recruitment of contralesional motor areas [6, 7] and the activation of secondary motor area [8, 9]. Moreover, from the perspective of functional and effective connectivity[10], the reorganization manifests the change of the pattern of the relation between two or in multiple brain regions. For examples, the inter-hemispheric functional connectivity between motor areas is correlated with the motor functions restoration during the recovery after stroke onset [11, 12], and the decreased bidirectional coupling between ipsilesional supplementary motor area and primary motor area has been found in the process of reorganization [13].

Despite the findings and advances in above studies, little is known about the dynamic change of brain networks linking to the integrative ability of the whole brain during reorganization. Wang *et al*. [14] have examined the changes of the motor executive network in the topological configuration during the recovery of stroke with graph theoretical analysis, which had been introduced as a novel approach to study functional networks in central nervous system [15]. The key finding of this study was that the motor executive network showed low efficiency of local information processing [16], suggesting that the motor executive network shifted towards a non-optimal network configuration with less functional segregation. Nevertheless, the reorganization of motor executive network with 21 motor-related brain regions is insufficient to reveal the change of the whole brain topological configuration during the recovery. With this consideration, we constructed brain-wide functional networks with 264 putative functional areas[17] based on the fMRI data of stroke patients when they were doing finger tapping task at four time points (i.e., within 10 days, around 2 weeks, 1 month, and 3 months) after stroke onset. Then the topological parameters (e.g., characteristic path length and cluster coefficient) of brain-wide functional networks were calculated using graph theoretical approaches, and statistical analysis was further performed to these parameters with linear mixed model. Based on these topological parameters at different time points, we can evaluate the change of efficiency of the global neural network, and thus offer new insights into the underlying mechanisms of motor function recovery after stroke.

II. MATERIALS AND METHODS

A. Subjects

Twelve stroke patients (male/female: 9/3; mean age: 61.5 years; age range: 47-77) were recruited for this study from the

* This work was supported by National Natural Science Foundation of China (No. 60901025, 61001015), National Basic Research Program of China (973 Program) (No. 2011CB013304), The International Science and Technology Cooperation Program of China (No.2011DFA10950), SJTU Funding for Innovation of Graduate Students. J. Sun is supported by 2011 SJTU SMC-Morning Star Award for Young Investigator.

L. Cheng (e-mail: smegel@sjtu.edu.cn), J. Sun (corresponding author; phone: +86-21-62933291; fax: +86-21-3420 4717; e-mail: jfsun@ sjtu.edu.cn), and S. Tong (e-mail: stong@ sjtu.edu.cn) are with the School of Biomedical Engineering, Shanghai Jiao Tong University, Shanghai, 200240, P. R. China.

Z. Wu (e-mail: wzy11549@rjh.com.cn) and F. Miao (e-mail: miaofei818@yahoo.com.cn) are with the Department of Neurology, Rui Jin Hospital, Shanghai Jiao Tong University School of Medicine, Shanghai, China.

Y. Fu (e-mail: fuyiki@sina.com) is with the Department of Radiology, Rui Jin Hospital, Shanghai Jiao Tong University School of Medicine, Shanghai, China.

L. Cheng and Z. Wu contributed equally to this work.

Rui Jin Hospital of Shanghai. All patients were with first-onset stroke and motor deficits according to Fugl-Meyer index (0-100, motor function is positive correlated to index). The average of Fugl-Meyer index of patients in the four time points, i.e., within 10 days, around 2 weeks, 1 month and 3 months after stroke onset, was 71.9, 72.8, 77.1, and 81.4, respectively. None of them had a history of neurological or psychiatric disorders. The patients were scanned by fMRI at four time points. From the second time point, some subjects dropped out in the follow-up scanning. The clinical data of patients are summarized in TABLE I. The Ethics Committee of Rui Jin Hospital approved this experiment and each participant gave informed consent.

TABLE I. PATIENT INFORMAITON AND THE MOTOR FUNCTIONAL SCORING AT FOUR TIME POINTS.

Subject No.	Gender	Fugl-Meyer Index(fMRI scanning)			
		<10 d	2 w	1 m	3 m
1	M	93 (√)	92 (√)	99 (√)	99 (√)
2	M	53 (√)	55 (√)	61 (√)	66 (√)
3	M	51 (√)	50	53(√)	57(√)
4	F	54 (√)	54 (√)	54	59
5	M	85 (√)	87 (√)	96	97
6	F	73 (√)	77 (√)	79	96
7	F	72 (√)	78 (√)	77 (√)	86 (√)
8	M	71 (√)	75 (√)	75	75
9	M	59 (√)	55	62	63
10	M	94 (√)	94 (√)	99 (√)	99 (√)
11	M	63 (√)	62 (√)	71 (√)	81 (√)
12	M	95 (√)	95 (√)	99 (√)	99

M=Male; F=Female; d=day; w=week; m=month; (√) indicates the subject had fMRI data in this time point

B. Task Design

The fMRI experiment was a block design consisting of rest status alternated with stimulation status for three repetitions (Fig. 1). At rest status, subjects were instructed to remain motionless, relaxing and awake; and when the stimulus was presented, subjects should do the finger-tapping task (touching thumb to each fingers as fast as possible). Both rest and stimulation status lasted for 30s.

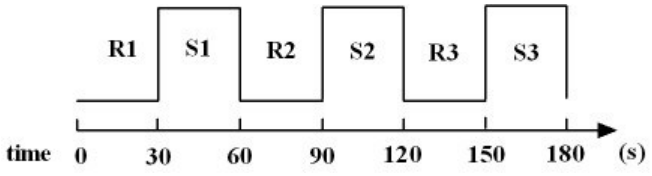

Figure 1. The block design of fMRI experiment. Rest status (R) alternated with stimulation status (S) for three repetitions.

C. Data Acquisition

All images were acquired on a 1.5 Tesla MRI scanner (Exicte HD, General Electric Medical System, Milwaukee, WI, USA). The head of each participant was snugly fixed by foam pad to reduce head movements and scanner noise. All fMRI data of the whole brain were acquired from the top of the brain to the lower part of the medulla oblongata, using an echo-planar imaging sequence: 32 axial slices, thickness/gap = 5/0 mm, matrix=64×64, repetition time=3000 ms, echo time=60 ms, flip angle=90°, field of view=240 mm×180 mm. The total scanning time is 3 min and 12 s in each experiment.

D. Preprocessing of fMRI Data

For each subject, the data of the first 12 s (4 volumes) were abandoned due to the magnetization equilibrium effects and the adaptation of the subjects to the circumstances. The rest fMRI data were preprocessed by SPM8 (http://www.fil.ion.ucl.ac.uk/spm) on MATLAB prior to the network analysis. The preprocessing included realignment, coregistration, normalization, and smoothing.

E. Construction of Brain-wide Functional Networks

First, we obtained the coordinates of putative functional 264 regions of interest (ROIs) based on the brain atlas proposed in Power's research by meta-analysis of ROIs and mapping of functional connectivity between ROIs[17]. The representative time series of each ROI was extracted by averaging the time series of voxels in the 10 mm diameter sphere around the predefined coordinates. Then, for each scan of each subject, Pearson's correlation coefficients of all pairs of the representative time series for 264 ROIs were calculated to obtain one symmetric correlation matrix. Finally, we converted each correlation matrix into an adjacency matrix, which represented a brain-wide functional network, by thresholding. Only those pairs of ROIs with correlation coefficients greater than the preset threshold were connected with edges. The corresponding elements of the adjacency matrix were set to "1" to represent the connection, while the corresponding elements of weight matrix were set to the absolute values of the correlation coefficients to denote the connection strength. We repeated the procedures for all correlation matrices, and built the weighted brain network for each subject at each fMRI scan point.

F. Graph Theoretical Analysis of Brain Network

Clustering coefficient and the characteristic path length are two basic parameters to character the local and the global topological properties of a network [18]. For a weighted graph, the weighted clustering coefficient of a node j is defined as

$$C_j^w = \frac{1}{s_j(k_j-1)} \sum_{(i,k)} \frac{w_{ij}+w_{ik}}{2} a_{ij} a_{ik} a_{jk} , \quad (1)$$

where s_j represents the strength of node j, which is defined as the sum of the weights w_{ij} of the edges connected to node j, k_j is generally called the node degree, which is the number of the edges connected to the node j, and a_{ij} is the element of adjacency matrix[19]. The clustering coefficient of the whole network is then defined as the average of the

clustering coefficient of all nodes. The weighted characteristic path length is defined as

$$L^w = \frac{N(N-1)}{\sum_{i=1}^{N}\sum_{j\neq i}^{N} 1/l_{ij}^w}, \qquad (2)$$

where l_{ij}^w represents the weighted shortest path length between node i and node j, and N represents the number of nodes in the network[20].

G. Statistical Analysis

In this study, a linear mixed model was adopted to estimate the changes of network parameters over time [21]. This model takes advantages of the data from each patient, including the patients with data that may miss at some time points in follow-up. The model is as follows,

$$Y_{ij} = \mu + b_i + X_{ij}\beta + \varepsilon_{ij}, \quad i = 1, 2, ..., K, \qquad (3)$$

where Y_{ij} denotes a parameter of the brain network for the jth scan of the ith patient, μ is the common intercept for all subjects, b_i is the random intercept for each patient, β is the scalar of fix effect, X_{ij} represents the logarithm of the value of time (in days) when the ith patient was scanned after stoke onset, ε_{ij} is the residual error of this model, and K is the number of patients. We estimated the parameters by the statistical analysis software Eviews6.

III. Results

We divided the patients into two groups according to the lesion location, i.e. the right hemisphere-damaged group (n=5), and the left hemisphere-damaged group (n=7). For each patient, we obtained the fMRI data for subjects while they were performing the finger-tapping task by the ipsilateral and the contralateral hands respectively at each time point. Therefore, in total we had four categories of functional networks corresponding to the fMRI data for: (i) right hemispheric stroke with contralateral finger tapping (denoted as RsTc networks)), (ii) right hemispheric stroke with ipsilateral finger tapping (denoted as RsTi networks), (iii) left hemispheric stroke with contralateral finger tapping (denoted as LsTc networks), and (iv) left hemispheric stroke with ipsilateral finger tapping (denoted as LsTi networks). The parameters for all the functional networks in four categories were calculated respectively.

The clustering coefficient and the characteristic path length quantify the local information processing efficiency and the global information transfer efficiency of a network, respectively. For the network in each category, the trends of the characteristic path length over time were examined by linear mixed model. Results showed that the characteristic path length of the RsTi networks increased significantly ($P<0.05$) with the recovery of stroke (Fig.2); however, no significant changes of the characteristic path length were found in other three categories of networks. Furthermore, the trends of the network clustering coefficients were investigated

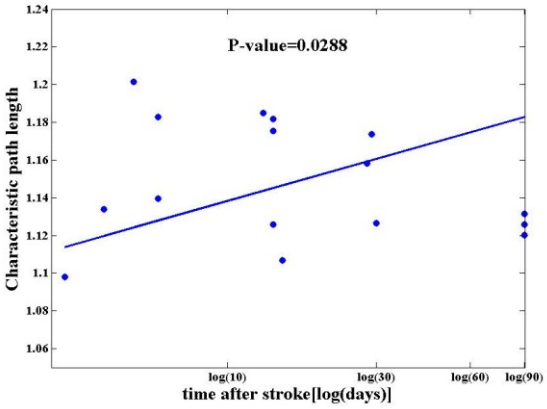

Figure 2. Scatter plot of the characteristic path length over time for networks constructed by fMRI data recorded for the right hemispheric stroke subjects during ipsilateral finger tapping task (denoted as RsTi networks). Y-axis value denotes the characteristic path length. X-axis value denotes the logarithm of the value of time (in days) after stroke. The normalized characteristic path length significantly increases with respect to time after stroke onset. This result was estimated by linear mixed model (Eq.3), where the estimated β corresponds to the slope of the line in this figure, and the estimated μ represents the intercept of the line.

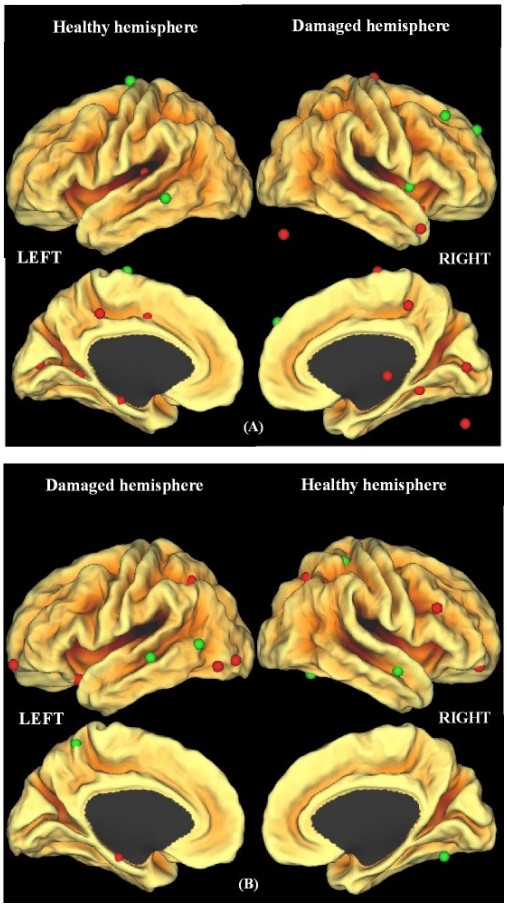

Figure 3. Illustration of nodes with significantly changed clustering coefficients. Red spheres denote the nodes whose clustering coefficients significantly decreased during recovery, and green spheres denote the nodes whose clustering coefficients significantly increased. (A) the right hemispheric stroke group, (B) the left hemispheric stroke group. Brain surface visualizations were created using Caret software and the PALS surface [22, 23].

as well, while no significant trends were observed during the recovery in all categories. In addition, we examined the clustering coefficients of every single node. The clustering coefficients of 26 nodes in the RsTc networks and 18 nodes in the LsTc networks were found to change (increased or decreased) significantly ($P<0.05$) over time, as demonstrated in Fig. 3. The increasing nodal clustering coefficients over time implied that the information processing efficiency increased in the corresponding local sub-networks.

IV. Discussion and Conclusion

The major findings in this study were (i) the characteristic path length increased over time, (ii) the clustering coefficient of network showed no significant change, while the clustering coefficients of some specific nodes changed (declined or increased) significantly (see the marked nodes in Fig. 3), when the brain underwent reorganization after the stroke onset. These results implied that the information processing efficiency in global network tended to decrease, while the information processing efficiency in some local sub-networks altered due to the reorganization during the recovery of stroke, which was in line with other studies [14, 24-26].

In conclusion, the brain-wide functional networks of 264 putative regions underwent reorganization during the stroke recovery, and shifted towards a non-optimal topological configuration. These findings based on graph theoretical analysis may broaden our knowledge about the functional reorganization of the brain during the recovery of stroke.

References

[1] P. W. Duncan, S. Min Lai, and J. Keighley, "Defining post-stroke recovery: implications for design and interpretation of drug trials," *Neuropharmacology,* vol. 39, pp. 835-841, 2000.

[2] M. Lotze, J. Markert, P. Sauseng, J. Hoppe, C. Plewnia, and C. Gerloff, "The role of multiple contralesional motor areas for complex hand movements after internal capsular lesion," *J Neurosci,* vol. 26, pp. 6096-102, May 31 2006.

[3] A. Feydy, R. Carlier, A. Roby-Brami, B. Bussel, F. Cazalis, L. Pierot, Y. Burnod, and M. A. Maier, "Longitudinal study of motor recovery after stroke: recruitment and focusing of brain activation," *Stroke,* vol. 33, pp. 1610-7, Jun 2002.

[4] D. Saur, R. Lange, A. Baumgaertner, V. Schraknepper, K. Willmes, M. Rijntjes, and C. Weiller, "Dynamics of language reorganization after stroke," *Brain,* vol. 129, pp. 1371-84, Jun 2006.

[5] Junfeng Sun, Shanbao Tong, and G.-Y. Yang, "Reorganization of Brain Networks in Aging and Age-related Diseases " *Aging and Disease,* vol. 3, 2011.

[6] H. Johansen-Berg, T. E. Behrens, M. D. Robson, I. Drobnjak, M. F. Rushworth, J. M. Brady, S. M. Smith, D. J. Higham, and P. M. Matthews, "Changes in connectivity profiles define functionally distinct regions in human medial frontal cortex," *Proc Natl Acad Sci U S A,* vol. 101, pp. 13335-40, Sep 7 2004.

[7] N. S. Ward, M. M. Brown, A. J. Thompson, and R. S. Frackowiak, "Neural correlates of motor recovery after stroke: a longitudinal fMRI study," *Brain,* vol. 126, pp. 2476-96, Nov 2003.

[8] S. C. Cramer, G. Nelles, R. R. Benson, J. D. Kaplan, R. A. Parker, K. K. Kwong, D. N. Kennedy, S. P. Finklestein, and B. R. Rosen, "A functional MRI study of subjects recovered from hemiparetic stroke," *Stroke,* vol. 28, pp. 2518-27, Dec 1997.

[9] E. A. Fridman, T. Hanakawa, M. Chung, F. Hummel, R. C. Leiguarda, and L. G. Cohen, "Reorganization of the human ipsilesional premotor cortex after stroke," *Brain,* vol. 127, pp. 747-58, Apr 2004.

[10] K. J. Friston, "Functional and effective connectivity in neuroimaging: A synthesis," *Human Brain Mapping,* vol. 2, pp. 56-78, 1994.

[11] B. J. He, A. Z. Snyder, J. L. Vincent, A. Epstein, G. L. Shulman, and M. Corbetta, "Breakdown of Functional Connectivity in Frontoparietal Networks Underlies Behavioral Deficits in Spatial Neglect," *Neuron,* vol. 53, pp. 905-918, 2007.

[12] M. P. van Meer, K. van der Marel, K. Wang, W. M. Otte, S. El Bouazati, T. A. Roeling, M. A. Viergever, J. W. Berkelbach van der Sprenkel, and R. M. Dijkhuizen, "Recovery of sensorimotor function after experimental stroke correlates with restoration of resting-state interhemispheric functional connectivity," *J Neurosci,* vol. 30, pp. 3964-72, Mar 17 2010.

[13] C. Grefkes, D. A. Nowak, S. B. Eickhoff, M. Dafotakis, J. Kust, H. Karbe, and G. R. Fink, "Cortical connectivity after subcortical stroke assessed with functional magnetic resonance imaging," *Ann Neurol,* vol. 63, pp. 236-46, Feb 2008.

[14] L. Wang, C. Yu, H. Chen, W. Qin, Y. He, F. Fan, Y. Zhang, M. Wang, K. Li, Y. Zang, T. S. Woodward, and C. Zhu, "Dynamic functional reorganization of the motor execution network after stroke," *Brain,* vol. 133, pp. 1224-38, Apr 2010.

[15] E. Bullmore and O. Sporns, "Complex brain networks: graph theoretical analysis of structural and functional systems," *Nat Rev Neurosci,* vol. 10, pp. 186-98, Mar 2009.

[16] D. S. Bassett and E. Bullmore, "Small-world brain networks," *Neuroscientist,* vol. 12, pp. 512-23, Dec 2006.

[17] J. D. Power, A. L. Cohen, S. M. Nelson, G. S. Wig, K. A. Barnes, J. A. Church, A. C. Vogel, T. O. Laumann, F. M. Miezin, B. L. Schlaggar, and S. E. Petersen, "Functional network organization of the human brain," *Neuron,* vol. 72, pp. 665-78, Nov 17 2011.

[18] D. J. Watts and S. H. Strogatz, "Collective dynamics of `small-world' networks," *Nature,* vol. 393, pp. 440-442, 1998.

[19] A. Barrat, M. Barthélemy, R. Pastor-Satorras, and A. Vespignani, "The architecture of complex weighted networks," *Proceedings of the National Academy of Sciences of the United States of America,* vol. 101, pp. 3747-3752, March 16, 2004 2004.

[20] S. Boccaletti, V. Latora, Y. Moreno, M. Chavez, and D. U. Hwang, "Complex networks: Structure and dynamics," *Physics Reports,* vol. 424, pp. 175-308, 2006.

[21] R. D. Gibbons, D. Hedeker, and S. DuToit, "Advances in analysis of longitudinal data," *Annu Rev Clin Psychol,* vol. 6, pp. 79-107, Apr 27 2010.

[22] D. C. Van Essen, "A Population-Average, Landmark- and Surface-based (PALS) atlas of human cerebral cortex," *Neuroimage,* vol. 28, pp. 635-62, Nov 15 2005.

[23] D. C. Van Essen, H. A. Drury, J. Dickson, J. Harwell, D. Hanlon, and C. H. Anderson, "An integrated software suite for surface-based analyses of cerebral cortex," *J Am Med Inform Assoc,* vol. 8, pp. 443-59, Sep-Oct 2001.

[24] F. Bartolomei, I. Bosma, M. Klein, J. C. Baayen, J. C. Reijneveld, T. J. Postma, J. J. Heimans, B. W. van Dijk, J. C. de Munck, A. de Jongh, K. S. Cover, and C. J. Stam, "Disturbed functional connectivity in brain tumour patients: Evaluation by graph analysis of synchronization matrices," *Clinical Neurophysiology,* vol. 117, pp. 2039-2049, 2006.

[25] M. Rubinov, S. A. Knock, C. J. Stam, S. Micheloyannis, A. W. Harris, L. M. Williams, and M. Breakspear, "Small-world properties of nonlinear brain activity in schizophrenia," *Hum Brain Mapp,* vol. 30, pp. 403-16, Feb 2009.

[26] C. J. Stam, W. de Haan, A. Daffertshofer, B. F. Jones, I. Manshanden, A. M. van Cappellen van Walsum, T. Montez, J. P. Verbunt, J. C. de Munck, B. W. van Dijk, H. W. Berendse, and P. Scheltens, "Graph theoretical analysis of magnetoencephalographic functional connectivity in Alzheimer's disease," *Brain,* vol. 132, pp. 213-24, Jan 2009.